

MFRNet: A New CNN Architecture for Post-Processing and In-loop Filtering

Di Ma, Fan Zhang, *Member, IEEE*, and David R. Bull, *Fellow, IEEE*

Abstract—In this paper, we propose a novel convolutional neural network (CNN) architecture, MFRNet, for post-processing (PP) and in-loop filtering (ILF) in the context of video compression. This network consists of four Multi-level Feature review Residual dense Blocks (MFRBs), which are connected using a cascading structure. Each MFRB extracts features from multiple convolutional layers using dense connections and a multi-level residual learning structure. In order to further improve information flow between these blocks, each of them also reuses high dimensional features from the previous MFRB. This network has been integrated into PP and ILF coding modules for both HEVC (HM 16.20) and VVC (VTM 7.0), and fully evaluated under the JVET Common Test Conditions using the Random Access configuration. The experimental results show significant and consistent coding gains over both anchor codecs (HEVC HM and VVC VTM) and also over other existing CNN-based PP/ILF approaches based on Bjøntegaard Delta measurements using both PSNR and VMAF for quality assessment. When MFRNet is integrated into HM 16.20, gains up to 16.0% (BD-rate VMAF) are demonstrated for ILF, and up to 21.0% (BD-rate VMAF) for PP. The respective gains for VTM 7.0 are up to 5.1% for ILF and up to 7.1% for PP.

Index Terms—Deep learning, CNN, in-loop filtering, post-processing, video compression, HEVC, VVC.

I. INTRODUCTION

IN recent years the consumption of video content has increased dramatically. This has been associated with demands for improved viewing quality, and for more immersive experiences (including augmented and virtual reality (AR and VR)) with multiple views, higher spatial and temporal resolutions and wider dynamic range, [1]. These all create pressure on network capacity and present significant challenges for video compression.

To address this, new video coding standards have been initiated including Versatile Video Coding (VVC) [2], Alliance for Open Media Video 1 and 2 (AV1/AV2) [3] and Essential Video Coding (EVC) [4]. All of these are expected to achieve significant coding gains compared to current standards [5, 6] such as High Efficiency Video Coding (HEVC) [7]. These new coding standards all employ a similar framework to that used in previous codecs such as H.264/AVC (Advanced Video Coding) [8], but with much more sophisticated modifications and enhancements. None of them however, exploit recent advances in artificial intelligence and machine learning.

The last decade has seen significant advances in the application of machine learning, especially using convolutional neural

networks (CNNs), for image and video analysis, recognition and processing [9]. More recently, deep learning techniques have also been applied to the problem of image and video compression, both to enhance existing coding modules and also to provide new end-to-end solutions [10, 11]. Amongst approaches that target specific coding modules, CNN-based post-processing (PP) and in-loop filtering (ILF) have delivered reductions in visual artefacts and overall improvements in perceptual quality, showing bit rate savings against codecs such as VVC. The coding gains reported are primarily for intra coding [12, 13], and the network architectures employed in many cases do not represent the latest deep learning advances.

In the above context, a new CNN architecture (MFRNet) is proposed for video compression, to enhance both post-processing and in-loop filtering. This employs Multi-level Feature review Residual dense Blocks (MFRB) in a cascading structure. The network was trained on a large database with diverse video content, and integrated into both HEVC (HM 16.20) and VVC (VTM 7.0) reference codecs. Results were evaluated on test sequences from the Joint Video Exploration Team (JVET) Common Test Conditions (CTC) [14] dataset using the Random Access configuration (the most effective default coding mode in HEVC and VVC). Significant improvements were observed over both HEVC and VVC test models and over other state-of-the-art CNN-based PP and ILF approaches. The proposed architecture also demonstrates superior performance when compared to other popular network structures.

The contributions of this paper are summarised below:

- 1) A novel CNN architecture is presented exploiting multi-level feature review residual dense blocks for post-processing and in-loop filtering.
- 2) This network has been integrated into both HEVC and VVC test models, demonstrating significant coding gains for Random Access configurations.
- 3) A comprehensive comparison is made between the proposed architecture and thirteen existing popular network structures, based on the same training and evaluation material.

The remainder of the paper is organised as follows. Section II reviews recent advances in video coding standards and the state of the art in deep video compression, in particular for post-processing and in-loop filtering. Section III describes the CNN-based PP/ILF coding modules, the proposed network architecture, and the training/evaluation processes, while Section IV reports experimental results with analysis and discussion. Finally, conclusions and future work are outlined in Section

D. Ma, F. Zhang and D. R. Bull are with the Department of Electrical and Electronic Engineering, University of Bristol, Bristol, BS8 1UB, UK (e-mail: di.ma@bristol.ac.uk; fan.zhang@bristol.ac.uk; dave.bull@bristol.ac.uk).

Manuscript submitted June 30, 2020.

V.

II. BACKGROUND

This section first overviews the latest standardisation activity for video compression (Section II-A), and reviews current applications of deep learning in the context of video compression (Section II-B). Section II-C describes the primary functions of post-processing (PP) and in-loop filtering (ILF), while Section II-D provides a brief summary of existing CNN-based PP and ILF approaches.

A. Video coding standards

Since the early 1980s, multiple generations of video coding standards have been developed by ITU-T and/or ISO/IEC for various application scenarios. Among these, the most successful has been H.264/AVC (Advanced Video Coding) [8] which was released in 2004 targeting Internet streaming and HDTV. H.264/AVC is still widely used, despite its successor HEVC/H.265 (High Efficiency Video Coding, 2013) [7] providing nearly 50% coding gain. In 2018, in order to provide improved support for immersive video formats (e.g. high dynamic range and 360°) with further compression efficiency improvements, a new coding standard, Versatile Video Coding (VVC) [2], was initiated. This is expected to be finalised in 2020 and currently [5] shows more than 35% overall coding gain over HEVC, but with a significant increase in encoder complexity.

In parallel with developments under ITU-T and ISO/IEC, the Alliance for Open Media (AOM, an industry consortium) has developed an open source and royalty-free coding solution, AOM Video 1 (AV1). AV1 was launched in 2018 to target Internet streaming and its most recent versions appear to offer evident and consistent performance improvements over HEVC [5, 15]. The development of its successor, AV2 (AOMedia Video 2) is also planned to start in 2020. Other recent advances in coding standards include the Essential Video Coding/MPEG-5 [4] and AVS standards [16] that target royalty free solutions and complexity-performance trade-offs.

B. Deep video compression

Inspired by recent advances in artificial intelligence, deep neural networks have started to play an important role in video compression to enhance individual coding tools including intra coding [17, 18], inter prediction [19, 20], transforms [21, 22], quantisation [23], entropy coding [24, 25], formats adaptation [26–28], post-processing (PP) [29, 30] and in-loop filtering (ILF) [31, 32]. Alternative deep learning coding architectures have also been proposed based on an end-to-end training and optimisation process [33–37]. More details on deep video compression can be found in this special issue and in [10, 11, 38].

For learning-based compression, in order to achieve good model generalisation and avoid potential over-fitting problems, it is essential for training material to include diverse content covering different formats and texture types. Existing learning-based coding methods often employ training databases developed for super-resolution [39], frame interpolation [40] or

classification [41]. More recently, a new extensive and representative video database, BVI-DVC, has been made available for training CNN-based coding tools [42]. This database has been shown to provide significant improvements in terms of coding gains over other commonly used training databases for various CNN architectures and coding modules (including PP and ILF).

C. PP and ILF in video coding

Following compression, decoded videos often exhibit noticeable visual artefacts including blocking discontinuities, ringing and blurring, and these become more evident as quantisation level increases. To reduce these distortions, post-processing can be employed at video decoder to improve reconstruction quality. When integrated into the encoding loop, filtered frames with fewer artefacts and improved quality can be used as reference for inter prediction [1].

In the latest version of VVC, the in-loop filtering module consists of three different stages including deblocking filtering (DBF), sample adaptive offset (SAO) and adaptive loop filtering (ALF). DBF is designed to adaptively suppress artefacts along block boundaries using low-pass smoothing filters according to discontinuity levels [43, 44]. SAO is invoked after DBF to make a non-linear adjustment that adds offsets to samples based on a look-up table created at the encoder using histogram analysis of signal amplitudes [45]. ALF is a new feature in VVC, which minimises distortions between the original and reconstructed blocks using an adaptively trained low-pass filter [46].

D. CNN-based PP and ILF

Deep neural networks, especially deep CNNs, have made significant contributions to single image super-resolution and image restoration. Common architectural features include (from simple to more complex): (i) Simple concatenated convolutional layers [47–49]; (ii) the addition of deeper residual blocks [50–54]; (iii) including dense connections [55, 56]; (iv) with cascading connections [57, 58]; and (v) with feature review structures [13, 59]. Notable examples of the use of CNNs for post-processing and in-loop filtering include [12, 13, 29–32, 59–70]. However, most of these methods do not employ advanced features such as residual dense blocks, cascading connections or feature review structures, and are often trained on relatively small databases [39, 71]. This can result in sub-optimal and/or non-generic models, and can only offer consistent coding gains for less effective coding configurations, such as All Intra (AI) and Low Delay (LD) modes in HEVC and VVC. For the case of the more commonly used Random Access (RA) configuration (which provides much higher coding efficiency than AI and LD) these existing CNN-based PP and ILF approaches, which employ simple network architectures, demonstrate little or no coding performance improvement.

III. PROPOSED ALGORITHM

This section presents the new CNN architecture, MFRNet, and describes how this is integrated into CNN-based post-processing (PP) and in-loop filtering (ILF) coding modules.

The training and evaluation methodologies are also provided in detail.

A. CNN-based PP and ILF coding modules

The CNN-based PP and ILF modules employed here are illustrated in Fig. 1 and 2. For the case of post-processing, the employed CNN filter is applied directly after the reconstructed frames are decoded from the transmitted bitstream, and produces a frame with improved reconstruction quality in the same format. As shown in Fig. 2, the CNN-based ILF module is located after the conventional in-loop filtering process, and has the same input and output format as for the PP case. This is similar to that for most of the previous contributions on CNN-based ILF filters [31, 68]. Compared to other possible designs, where the CNN operation is not performed as the last step in the whole coding workflow (e.g. before ALF, SAO or DBF), this implementation will not conflict with the existing conventional loop filters and will achieve better reconstruction performance due to its end-to-end optimisation in the training process.

B. Proposed CNN architecture

The CNN architecture proposed for PP and ILF is illustrated in Fig. 3-5. This network accepts a 96×96 YCbCr 4:4:4 image block as input, and outputs a filtered image block in the same format. It first employs a convolutional layer alongside a Leaky ReLU (LReLU) activation function to extract shallow features (SFs) from the input image block. This SF extraction layer is followed by four Multi-level Feature review Residual dense Blocks (MFRBs, B_1 - B_4), which are designed for deep dense feature extraction. Ten cascading connections, shown as black curves in Fig. 3, are utilised to feed the initial SFs and the output from the first three MFRBs (G_1 , G_2 and G_3) into following MFRBs or into the first reconstruction layer (shown as RL1 in Fig. 3) through a 1×1 convolutional layer (with 1 LReLU). This structure is designed to effectively improve information flow while reducing the number of residual dense blocks in the network [57, 58]. Moreover, each of the first three MFRBs also feeds its high dimensional feature outputs, F_1 , F_2 , F_3 , into the next MFRB, as shown in Fig. 4, in order to reuse previous HDFs [55]. After four MFRBs and the first reconstruction layer (RL1), a skip connection is employed to connect the output of this reconstruction layer and the output of the shallow feature extraction layer. Finally, an additional reconstruction layer (RL2) and an output layer are employed to output a residual signal, which is then combined with the input through a long skip connection to obtain the final image block. The kernel sizes, feature map numbers and stride values for each convolution layer can be found in Fig. 3.

Fig. 4 shows the structure of each MFRB (B_i , $i=1, 2, 3$ and 4), which contains three Feature review Residual dense Blocks (FRBs), b_i^1 , b_i^2 and b_i^3 . In many existing CNN architectures, which employ residual (or residual dense) blocks [50, 52, 54–56], there is only a single information flow, which prevents high level blocks from fully accessing previously generated features. This leads to a problem of diminishing feature reuse, which in turn affects the overall performance of the network

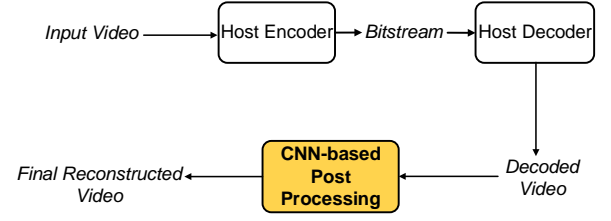


Fig. 1: Coding workflow with a CNN-based PP module.

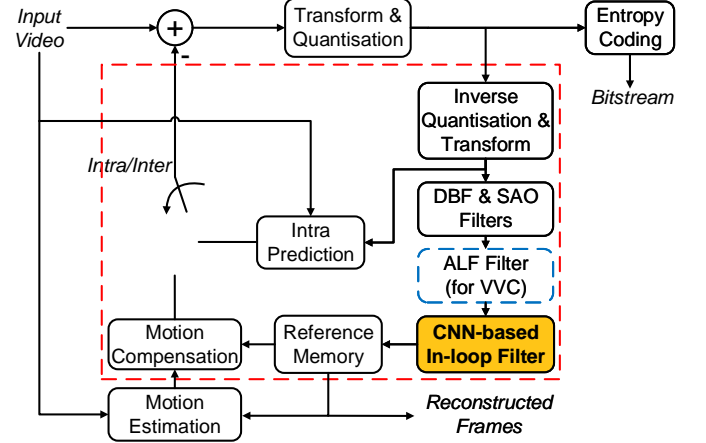


Fig. 2: Coding workflow with a CNN-based ILF module (the modules in the dashed box form the corresponding decoder).

[13]. To address this issue, in the proposed architecture, each FRB (b_i^j), except the first one in B_1 and the last one in B_4 , is designed to have two inputs and two outputs [13], as shown in Fig. 4 and 5. Each FRB not only receives the main branch output from the previous MFRB (G_{i-1}) or FRB (g_i^{j-1}), but also accepts the side branch output from the previous MFRB (F_{i-1}) or FRB (f_i^{j-1}), which contains high dimensional features. Respectively, in addition to its main branch output (γ_i^j), each FRB also feeds its side branch output (f_i^j) into the subsequent FRB block in this or the next MFRB (if applicable). This new structure allows each FRB to review the high dimensional features generated in its previous block, which effectively enhances the information flow between blocks. Finally, a multi-level residual learning structure is designed to apply skip connection between the input of the first FRB and the output of each FRB. This enables bypassing of redundant information and stabilises training and evaluation processes [72, 73].

Fig. 5 shows the FRB structure (b_i^j), which contains a main branch and a side branch. The former first accepts the output from the previous MFRB (G_{i-1}) or FRB (g_i^{j-1}) if it is available, and extracts dense features through four convolutional layers with dense connections [55, 74]. Each of these layers contains one convolutional layer and a LReLU function. The output of these four dense convolutional layers are then concatenated together with the side branch output from the previous MFRB (F_{i-1}) or FRB (f_i^{j-1}) and fed into the last convolutional layer. The output of this layer is combined with the input (G_{i-1} or g_i^{j-1}) of this FRB through

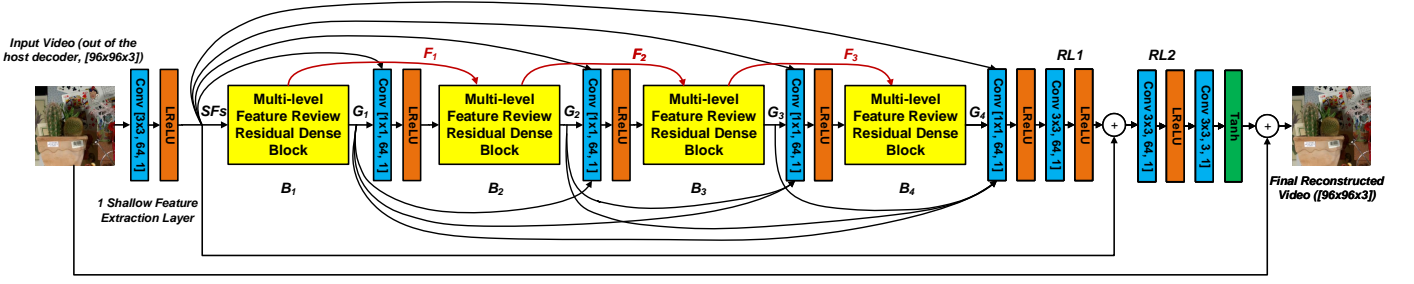


Fig. 3: Illustration of the proposed MFRNet architecture.

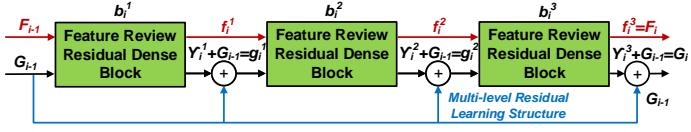


Fig. 4: Illustration of an MFRB (B_i).

a skip connection to obtain the final FRB output (g_i^j). The concatenated, high dimensional features (HDFs) are further fed into two modified residual blocks and one convolutional layer with a 1×1 kernel size to obtain the output of this side branch (f_i^j) in this FRB. This is also sent to the subsequent FRB block (if applicable) to realise HDF reviewing.

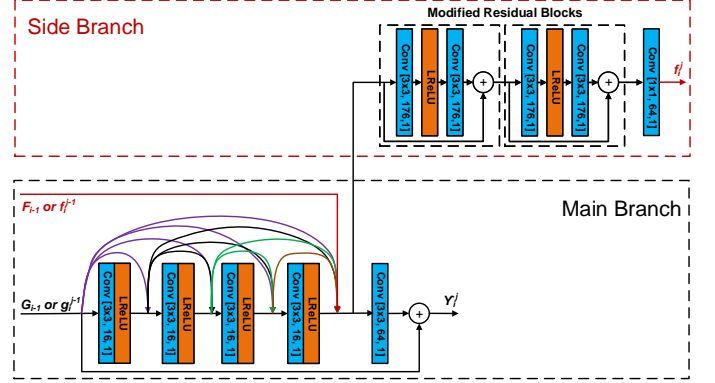


Fig. 5: Illustration of an FRB (b_i^j).

C. Network training and evaluation

As mentioned in Section II, training databases are critical for optimising the performance of learning-based compression algorithms. In this work, a large video database, BVI-DVC [42], is employed to generate training material. This database contains 800 carefully selected video sequences, all of which have 64 frames with 10 bit and YCbCr 4:2:0 format at four different resolutions from 270p to 2160p. These sequences were compressed by HEVC HM 16.20 and VVC VTM 7.0 codecs using the JVET-CTC Random Access (RA) configuration with four QP values: 22, 27, 32 and 37. During encoding and decoding, all default in-loop filters within the HM and VTM codecs were kept active. For each QP, compressed video frames and their corresponding original counterparts were randomly selected, segmented into 96×96 image blocks, and converted to YCbCr 4:4:4 format. During this process, block rotation was applied to achieve data augmentation. This results in approximately 192,000 pairs of blocks for each QP group.

The proposed CNN was implemented and trained using the TensorFlow (version 1.8.0) framework with the following training parameters: ℓ_1 as loss function; Adam optimisation [75] with hyper-parameters of $\beta_1=0.9$ and $\beta_2=0.999$; batch size of 16; 200 training epochs; learning rate of 0.0001; weight decay of 0.1 for every 100 epochs.

Based on the generated training content, four CNN models (aligned with the four QP groups) were trained for each codec (HM 16.20 and VTM 7.0), which are subsequently used in the

evaluation stage for different base QP values:

$$\text{CNN Models} = \begin{cases} \text{Model}_1, & \text{QP}_{\text{base}} \leq 24.5 \\ \text{Model}_2, & 24.5 < \text{QP}_{\text{base}} \leq 29.5 \\ \text{Model}_3, & 29.5 < \text{QP}_{\text{base}} \leq 34.5 \\ \text{Model}_4, & \text{QP}_{\text{base}} > 34.5 \end{cases} \quad (1)$$

When the trained CNN models are used for post-processing and in-loop filtering, each reconstructed frame is segmented into 96×96 overlapping blocks with an overlap size of 4 pixels, and converted to YCbCr 4:4:4 format. The CNN output image blocks are then converted to the original format and aggregated in the same way to form the final video frame.

IV. RESULTS AND DISCUSSION

All of the enhanced codecs have been fully tested under the JVET Common Test Conditions (CTC) using the Random Access configuration (Main10 profile) with four QP values (22, 27, 32 and 37). As discussed in Section I and Section II, in order to prove the effectiveness of the proposed CNN architecture, all of the experiments were conducted using the Random Access configuration, which offers significantly better coding efficiency compared to the All Intra and Low Delay modes. Nineteen test sequences from JVET CTC SDR (standard dynamic range) classes A1, A2, B, C and D were used as test material. None of these sequences are included in the training database. The original HM 16.20 and VTM 7.0 codecs are employed as benchmark anchors for all tested approaches, and rate quality performance is measured using the Bjontegaard Delta [76] methods based on two quality metrics,

TABLE I: Compression results of the MFRNet-based ILF and PP for HM 16.20.

Class-Sequence	CNN-based In-loop Filtering (<i>Full Test</i>)				CNN-based Post-Processing			
	BD-rate (PSNR)	BD-PSNR	BD-rate (VMAF)	BD-VMAF	BD-rate (PSNR)	BD-PSNR	BD-rate (VMAF)	BD-VMAF
A1-Campfire	-6.2%	+0.12dB	-16.5%	+1.33	-12.4%	+0.22dB	-19.2%	+1.61
A1-FoodMarket4	-8.6%	+0.29dB	-17.1%	+1.57	-11.1%	+0.37dB	-20.6%	+1.91
A1-Tango2	-11.9%	+0.17dB	-21.6%	+1.91	-15.1%	+0.21dB	-25.2%	+2.09
A2-CatRobot1	-12.6%	+0.23dB	-21.5%	+1.73	-17.5%	+0.33dB	-29.0%	+2.08
A2-DaylightRoad2	-17.1%	+0.21dB	-25.3%	+1.82	-21.4%	+0.27dB	-31.8%	+2.00
A2-ParkRunning3	-6.8%	+0.28dB	-11.9%	+1.32	-8.9%	+0.37dB	-12.1%	+1.36
Class A (2160p)	-10.5%	+0.22dB	-19.0%	+1.61	-14.4%	+0.30dB	-23.0%	+1.84
B-BasketballDrive	-12.4%	+0.30dB	-11.7%	+0.92	-14.8%	+0.35dB	-19.5%	+1.50
B-BQTerrace	-16.5%	+0.23dB	-25.5%	+0.67	-20.7%	+0.29dB	-29.9%	+0.50
B-Cactus	-13.2%	+0.31dB	-16.0%	+1.34	-14.6%	+0.34dB	-21.7%	+1.63
B-MarketPlace	-7.3%	+0.22dB	-14.9%	+1.64	-9.6%	+0.30dB	-19.7%	+2.05
B-RitualDance	-6.0%	+0.29dB	-13.8%	+1.57	-10.7%	+0.53dB	-18.3%	+2.15
Class B (1080p)	-11.1%	+0.27dB	-16.4%	+1.23	-14.1%	+0.36dB	-21.8%	+1.57
C-BasketballDrill	-9.4%	+0.42dB	-8.1%	+0.90	-14.4%	+0.65dB	-16.1%	+1.86
C-BQMall	-10.8%	+0.44dB	-12.9%	+0.82	-13.6%	+0.56dB	-20.9%	+1.39
C-PartyScene	-7.3%	+0.31dB	-14.7%	+1.44	-13.6%	+0.59dB	-19.9%	+1.91
C-RaceHorses	-7.8%	+0.30dB	-12.5%	+1.02	-10.2%	+0.39dB	-15.8%	+1.41
Class C (480p)	-8.8%	+0.37dB	-12.1%	+1.05	-13.0%	+0.55dB	-18.2%	+1.64
D-BasketballPass	-8.8%	+0.45dB	-11.9%	+1.58	-12.3%	+0.64dB	-13.9%	+1.87
D-BlowingBubbles	-7.4%	+0.31dB	-12.5%	+1.26	-11.6%	+0.49dB	-17.9%	+1.79
D-BQSquare	-14.9%	+0.56dB	-23.6%	+1.05	-24.1%	+0.92dB	-32.5%	+1.48
D-RaceHorses	-9.0%	+0.44dB	-13.1%	+1.32	-10.7%	+0.53dB	-15.0%	+1.62
Class D (240p)	-10.0%	+0.44dB	-15.3%	+1.30	-14.7%	+0.65dB	-19.8%	+1.69
Overall	-10.2%	+0.30dB	-16.0%	+1.30	-14.1%	+0.40dB	-21.0%	+1.70

Peak Signal-to-Noise-Ratio (PSNR, luminance channel only) and Video Multimethod Assessment Fusion (VMAF, version 0.6.1) [77]. PSNR is widely used as a quality metric for image and video compression while VMAF is a learning-based assessment method, which combines multiple quality metrics and video features using a Support Vector Machine (SVM) regressor. The latter has been shown to offer better correlation performance with subjective opinions on compressed content [78]. It is also noted that during the evaluation stage, the original in-loop filters in both HM and VTM remain enabled throughout the coding process for all test cases. The training and evaluation processes were both executed on a shared cluster, BlueCrystal Phase 4 (BC4) based in the University of Bristol [79], in which each node contains two 14 core 2.4 GHz Intel E5-2680 V4 (Broadwell) CPUs, 128 GB of RAM, and NVIDIA P100 GPU devices.

A. Compression performance

TABLE I and II summarise the compression performance of the PP and ILF coding modules (with the proposed CNN) when integrated into HEVC HM 16.20 and VVC VTM 7.0. It can be observed that our proposed approach achieves significant and consistent coding gains on all test sequences when integrated into HEVC, with average BD-rates of -10.2% and -14.1% for PP and ILF respectively. The coding gains are reduced for VTM, but are still significant with average BD-rates of -4.6% and -6.7% for ILF and PP respectively based on the assessment of PSNR. It can also be seen that, for both

host codecs and both tested coding modules, the bitrate savings according to VMAF are generally higher than those for PSNR.

As shown in TABLE I and II, the coding gains for PP are consistently higher than those for ILF, by approximately 2% for VTM and 4-5% for HM (in terms of BD-rate). This may at first appear surprising but it should be remembered that, unlike conventional post processing, CNN-based PP does employ end-to-end training. In addition, when CNN-processed frames are employed as a reference (after in-loop filtering), they are used to predict subsequently encoded frames through motion estimation and compensation. This process has not been reflected in the current CNN training (i.e. with CNN-processed content as network input), and is likely to cause the CNN-based filter to become less effective. Similar results have been observed by other authors when the same CNN is employed for both PP and ILF [64]¹.

B. Comparison between CNN-based PP and ILF approaches

The coding performance of the proposed CNN model is compared here with other notable CNN-based PP and ILF methods developed for the HEVC and VVC Random Access configuration. These include [12, 29, 31, 32, 59, 59–61, 64–67, 70, 80]². It should be noted that these approaches have not

¹It is also noted that, in TABLE III, the ILF results are better than PP for [12, 59]. This is because these CNN models employed for PP have been re-trained using data that is different [29] to that in their original literature.

²It is noted that [80] has been commonly used as a benchmark for ILF approaches, although it is not a CNN-based solution. We have included it here due to its consistent performance and popularity.

TABLE II: Compression results of the MFRNet-based ILF and PP for VTM 7.0.

Class-Sequence	CNN-based In-loop Filtering (<i>Full Test</i>)				CNN-based Post-Processing			
	BD-rate (PSNR)	BD-PSNR	BD-rate (VMAF)	BD-VMAF	BD-rate (PSNR)	BD-PSNR	BD-rate (VMAF)	BD-VMAF
A1-Campfire	-4.5%	+0.07dB	-8.3%	+0.52	-6.8%	+0.10dB	-10.3%	+0.67
A1-FoodMarket4	-3.5%	+0.10dB	-7.3%	+0.49	-5.0%	+0.14dB	-9.0%	+0.68
A1-Tango2	-5.9%	+0.07dB	-6.2%	+0.40	-8.4%	+0.09dB	-7.1%	+0.52
A2-CatRobot1	-6.7%	+0.10dB	-6.5%	+0.36	-9.3%	+0.13dB	-9.0%	+0.51
A2-DaylightRoad2	-7.6%	+0.07dB	-8.3%	+0.32	-9.5%	+0.09dB	-10.0%	+0.32
A2-ParkRunning3	-1.5%	+0.06dB	-3.1%	+0.27	-2.7%	+0.11dB	-3.5%	+0.38
Class A (2160p)	-5.0%	+0.08dB	-6.6%	+0.39	-7.0%	+0.11dB	-8.2%	+0.51
B-BasketballDrive	-4.3%	+0.09dB	-5.5%	+0.31	-7.2%	+0.15dB	-6.2%	+0.44
B-BQTerrace	-6.9%	+0.09dB	-5.2%	+0.10	-8.1%	+0.10dB	-7.2%	+0.33
B-Cactus	-4.4%	+0.09dB	-5.4%	+0.34	-6.7%	+0.13dB	-7.5%	+0.51
B-MarketPlace	-3.3%	+0.09dB	-4.4%	+0.35	-4.4%	+0.12dB	-5.9%	+0.51
B-RitualDance	-2.8%	+0.13dB	-3.9%	+0.38	-5.2%	+0.24dB	-6.3%	+0.66
Class B (1080p)	-4.3%	+0.10dB	-4.9%	+0.30	-6.3%	+0.15dB	-6.6%	+0.49
C-BasketballDrill	-4.4%	+0.18dB	-1.7%	+0.20	-6.7%	+0.28dB	-4.8%	+0.53
C-BQMall	-4.2%	+0.15dB	-5.5%	+0.28	-7.4%	+0.27dB	-7.8%	+0.45
C-PartyScene	-2.0%	+0.08dB	-3.4%	+0.19	-6.1%	+0.25dB	-5.4%	+0.40
C-RaceHorses	-2.5%	+0.09dB	-5.4%	+0.37	-3.7%	+0.13dB	-5.7%	+0.47
Class C (480p)	-3.3%	+0.13dB	-4.0%	+0.26	-6.0%	+0.23dB	-5.9%	+0.46
D-BasketballPass	-6.2%	+0.30dB	-4.6%	+0.48	-7.4%	+0.37dB	-5.5%	+0.67
D-BlowingBubbles	-4.6%	+0.19dB	-3.6%	+0.25	-5.9%	+0.24dB	-5.2%	+0.43
D-BQSquare	-6.6%	+0.24dB	-3.1%	+0.12	-11.5%	+0.41dB	-12.4%	+0.25
D-RaceHorses	-4.6%	+0.21dB	-5.6%	+0.47	-5.7%	+0.27dB	-5.9%	+0.58
Class D (240p)	-5.5%	+0.24dB	-4.2%	+0.33	-7.6%	+0.32dB	-7.3%	+0.48
Overall	-4.6%	+0.10dB	-5.1%	+0.30	-6.7%	+0.20dB	-7.1%	+0.50

been re-implemented due primarily to a lack of their source code. Instead their compression results are extracted directly from the corresponding literature..

TABLE III and IV summarise BD-rate (PSNR) results for five PP and five ILF methods (described above) for each host codec (HM and VTM) and compare with our approach. Due to the limitations of results available in the literature, only results for Class C and D are compared for HEVC HM. It can be observed that, for both host codecs and for the two coding modules, when MFRNet is integrated into PP and ILF modules, it significantly outperforms competing methods, and the improvements are consistent across content classes. This is likely due to the advanced structures employed in the proposed MFRNet architecture and the diversity of the training content used.

C. Comparisons with other popular CNN architectures

To further demonstrate the effectiveness of the proposed MFRNet CNN structure, we have also compared it with thirteen popular CNN architectures in the context of PP and ILF for HEVC HM. These include SRCNN [47], Highway Networks [81, 82], FSRCNN [48], VDSR [49], DRRN [50], EDSR [51], SRResNet [52], ESRRResNet [56], CARN [57], RCAN [53], RDN [55], MSRRResNet [54] and U²-Net [83]. Most of these models have been widely used in image super-resolution and restoration, and some (VDSR and MSRRResNet) have also been utilised in CNN-based video compression tools [27, 54, 62, 84]. Most of these approach provided superior

performance to the state of the art in their application domain when they were first proposed.

All thirteen models have been re-implemented using the same framework (TensorFlow 1.8.0) and were integrated into PP and ILF coding modules for HEVC HM 16.20. During re-implementation, the input and output interfaces of these networks have been modified to satisfy the data format requirements. All networks were also trained on the BVI-DVC database following the same methodology as for the proposed network, using loss functions as described in their original literature. Evaluation results on all 19 JVET test sequences are summarised in TABLE V and compared to those for MFRNet. The original HEVC HM 16.20 is employed as a benchmark. It should be noted that a *Short Test* was conducted for evaluating different ILF coding modules as described in JVET proposal M0904 [85], in which only the first intra period of each test sequence was encoded, while a *Full Test* (processing all frames in the sequence) was applied for PP. The relative computational complexity for each approach has also been calculated and benchmarked against the original HEVC HM 16.20 encoder (for ILF) and decoder (for PP).

It can be observed that MFRNet offers the best performance for both PP and ILF when compared to the other thirteen architectures, with average coding gains of 14.1% for PP and 9.9% for ILF based on PSNR, and 21.0% for PP and 15.6% for ILF according to VMAF. These figures are consistently greater than those for other networks. In contrast, the computational complexity of the proposed architecture is lower than that of Highway Networks, RCAN, EDSR, ESRRResNet and RDN.

TABLE III: Comparison between MFRNet-based PP and ILF and existing CNN-based PP and ILF approaches for HEVC.

Compression Performance Comparisons for Post-Processing Tools (HEVC HM)						
Sequence (Class)	[12] (HM 16.9)	[59] (HM 16.15)	[60] (HM 16.0)	[61] (HM 16.19)	[29] (HM 16.0)	Proposed Method (HM 16.20)
	BD-rate (PSNR)	BD-rate (PSNR)	BD-rate (PSNR)	BD-rate (PSNR)	BD-rate (PSNR)	BD-rate (PSNR)
Class C (480p)	0.63%	-2.6%	-6.8%	-6.6%	-7.1%	-13.0%
Class D (240p)	1.73%	-2.6%	-8.0%	-4.8%	-7.3%	-14.7%
Overall	1.2%	-2.6%	-7.4%	-5.7%	-7.2%	-13.9%
Compression Performance Comparisons for In-loop Filtering Tools (HEVC HM)						
Sequence (Class)	[80] (HM 16.5)	[12] (HM 16.9)	[59] (HM 16.15)	[31] (HM 12.0)	[32] (HM 16.9)	Proposed Method (HM 16.20)
	BD-rate (PSNR)	BD-rate (PSNR)	BD-rate (PSNR)	BD-rate (PSNR)	BD-rate (PSNR)	BD-rate (PSNR)
Class C (480p)	-4.6%	-3.0%	-3.9%	-7.1%	-4.5%	-8.8%
Class D (240p)	-2.5%	-2.3%	-4.6%	-4.4%	-3.3%	-10.0%
Overall	-3.6%	-2.7%	-4.3%	-5.8%	-3.9%	-9.4%

TABLE IV: Comparison between MFRNet-based PP and ILF and existing CNN-based PP and ILF approaches for VVC.

Compression Performance Comparisons for Post-Processing Tools (VVC VTM)						
Sequence (Class)	[64] (VTM 5.0)	[65] (VTM 5.0)	[66] (VTM 5.0)	[67] (VTM 5.0)	[30] (VTM 4.0.1)	Proposed Method (VTM 7.0)
	BD-rate (PSNR)	BD-rate (PSNR)	BD-rate (PSNR)	BD-rate (PSNR)	BD-rate (PSNR)	BD-rate (PSNR)
Class A (2160p)	-2.0%	-1.3%	-1.2%	-0.2%	-3.3%	-7.0%
Class B (1080p)	-1.3%	-1.5%	0.4%	-0.2%	-2.6%	-6.3%
Class C (480p)	0.3%	-3.3%	2.2%	-0.6%	-3.9%	-6.0%
Class D (240p)	N/A	-5.0%	6.6%	-0.8%	-5.8%	-7.6%
Overall	-1.2%	-2.6%	1.6%	-0.4%	-3.8%	-6.7%
Compression Performance Comparisons for In-loop Filtering Tools (VVC VTM)						
Sequence (Class)	[68] (VTM 5.0)	[64] (VTM 5.0)	[65] (VTM 5.0)	[69] (VTM 5.0)	[70] (VTM 4.0)	Proposed Method (VTM 7.0)
	BD-rate (PSNR)	BD-rate (PSNR)	BD-rate (PSNR)	BD-rate (PSNR)	BD-rate (PSNR)	BD-rate (PSNR)
Class A (2160p)	-2.0%	-1.7%	-0.4%	-1.3%	N/A	-5.0%
Class B (1080p)	-1.4%	-0.6%	0.6%	-0.8%	-1.5%	-4.3%
Class C (480p)	0.2%	0.3%	-1.2%	-0.9%	-3.1%	-3.3%
Class D (240p)	N/A	N/A	-3.1%	-0.8%	-3.9%	-5.5%
Overall	-1.2%	-0.8%	-0.9%	-1.0%	-2.7%	-4.6%

D. Complexity analysis

Finally, the complexity figures of the MFRNet-based ILF and PP are presented in TABLE VI. It can be observed that, due to the integration of MFRNet, the encoding complexity (for ILF) is on average 5.3 and 2.4 times comparing to original HEVC HM 16.20 and VVC VTM 7.0 respectively. When the proposed network is employed for post-processing at the decoder, the average decoding time is 81.2 times that of HM and 72.6 times that of VTM.

V. CONCLUSION

In this paper, a new CNN architecture, MFRNet, has been proposed as a means of enhancing post-processing (PP) and

in-loop filtering (ILF) in the context of video compression. MFRNet comprises four multi-level feature review residual dense blocks, and employs a cascading structure to improve information flow. Each of these block is designed to have a dense connection structure to extract features from multiple convolutional layers, and it can also reuse high dimensional features from the previous block. The proposed CNN has been integrated into PP and ILF modules for both HEVC and VVC standard codecs, and has been fully evaluated using the JVET standard test sequences. The results demonstrate significant coding gains, with a 16.0% improvement for ILF and 21.0% for PP over HM 16.20 in terms of VMAF, and a corresponding 5.1% for ILF and 7.1% for PP against VTM 7.0. Further

TABLE V: Comparison between thirteen popular CNN architectures and the proposed MFRNet in the context of ILF and PP.

CNN Model	CNN-based In-loop Filtering (<i>Short Test</i>)			CNN-based Post-Processing		
	BD-rate	BD-rate	Relative Complexity	BD-rate	BD-rate	Relative Complexity
	(PSNR)	(VMAF)	(Encoding)	(PSNR)	(VMAF)	(Decoding)
SRCNN [47]	-1.4%	-8.5%	1.2×	-1.9%	-7.4%	26.5×
FSRCNN [48]	-1.3%	-8.1%	1.5×	-1.6%	-7.3%	36.2×
VDSR [49]	-2.2%	-6.5%	1.8×	-1.9%	-7.6%	54.3×
DRRN [50]	-6.8%	-11.0%	2.4×	-10.8%	-14.9%	71.6×
EDSR [51]	-5.9%	-9.9%	9.4×	-10.0%	-14.6%	119.3×
SRResNet [52]	-6.4%	-10.6%	2.0×	-9.8%	-12.7%	64.9×
MSRResNet [54]	-6.4%	-11.3%	2.1×	-10.4%	-14.2%	65.1×
CARN [57]	-6.9%	-11.1%	1.9×	-11.2%	-15.4%	59.2×
U ² -Net [83]	-7.1%	-11.2%	3.3×	-11.5%	-15.9%	80.2×
ESRResNet [56]	-7.3%	-12.0%	7.8×	-11.8%	-17.7%	101.1×
Highway Networks [81, 82]	-7.2%	-12.7%	8.6×	-12.0%	-18.1%	117.2×
RCAN [53]	-7.4%	-11.4%	12.4×	-12.1%	-18.5%	127.6×
RDN [55]	-7.5%	-11.8%	5.7×	-12.2%	-17.0%	91.8×
MFRNet	-9.9%	-15.6%	5.3×	-14.1%	-21.0%	81.2×

TABLE VI: Relative Complexity of the MFRNet-based ILF and PP.

Hose Codec	HEVC HM 16.20		VVC VTM 7.0	
	ILF (Encoding)	PP (Decoding)	ILF (Encoding)	PP (Decoding)
Class A (2160p)	1.3×	27.3×	1.1×	23.7×
Class B (1080p)	3.9×	51.5×	1.3×	47.2×
Class C (480p)	8.2×	118.7×	2.1×	101.4×
Class D (240p)	10.3×	161.7×	6.1×	148.9×
Average	5.3×	81.2×	2.4×	72.6×

comparisons have shown the superiority of the MFRNet architecture over other existing popular deep networks, and over other reported CNN-based PP/ILF approaches. Future work will investigate enhanced ILF training strategies and reductions in computational complexity of the proposed network.

REFERENCES

- [1] D. R. Bull, *Communicating pictures: A course in Image and Video Coding*, Academic Press, 2014.
- [2] B. Bross, J. Chen, S. Liu, and Y.-K. Wang, "Versatile Video Coding (Draft 10)," in *JVET-S2001. ITU-T and ISO/IEC*, 2020.
- [3] AOMedia Video 1 (AV1), "https://aomedia.googlesource.com/."
- [4] K. Choi, J. Chen, D. Rusanovskyy, K.-P. Choi, and E. S. Jang, "An overview of the MPEG-5 Essential Video Coding standard [standards in a nutshell]," *IEEE Signal Processing Magazine*, vol. 37, no. 3, pp. 160–167, 2020.
- [5] F. Zhang, A. V. Katsenou, M. Afonso, G. Dimitrov, and D. R. Bull, "Comparing VVC, HEVC and AV1 using objective and subjective assessments," *arXiv preprint arXiv:2003.10282*, 2020.
- [6] P. Topiwala, M. Krishnan, and W. Dai, "Performance comparison of VVC, AV1 and EVC," in *Applications of Digital Image Processing XLII*. International Society for Optics and Photonics, 2019, vol. 11137, p. 1113715.
- [7] ITU-T Rec. H.265, "High Efficiency Video Coding," ITU-T Std., (2015).
- [8] ITU-T Rec. H.264, "Advanced Video Coding for generic audiovisual services," ITU-T Std., (2005).
- [9] G. Yao, T. Lei, and J. Zhong, "A review of convolutional-neural-network-based action recognition," *Pattern Recognition Letters*, vol. 118, pp. 14–22, 2019.
- [10] S. Ma, X. Zhang, C. Jia, Z. Zhao, S. Wang, and S. Wanga, "Image and video compression with neural networks: A review," *IEEE Transactions on Circuits and Systems for Video Technology*, 2019.
- [11] D. Liu, Y. Li, J. Lin, H. Li, and F. Wu, "Deep learning-based video coding: A review and a case study," *ACM Computing Surveys (CSUR)*, vol. 53, no. 1, pp. 1–35, 2020.
- [12] Y. Dai, D. Liu, and F. Wu, "A convolutional neural network approach for post-processing in HEVC intra coding," in *International Conference on Multimedia Modeling*. Springer, 2017, pp. 28–39.
- [13] D. Wang, S. Xia, W. Yang, Y. Hu, and J. Liu, "Partition tree guided progressive rethinking network for in-loop filtering of HEVC," in *2019 IEEE International Conference on Image Processing (ICIP)*. IEEE, 2019, pp. 2671–2675.
- [14] F. Bossen, J. Boyce, X. Li, V. Seregin, and K. Suhring, "JVET common test conditions and software reference configurations for SDR video," in *the JVET meeting*. ITU-T, ISO/IEC, 2019, number JVET-M1001.
- [15] Y. Chen, D. Mukherjee, J. Han, A. Grange, Y. Xu, S. Parker, C. Chen, H. Su, U. Joshi, C.-H. Chiang, et al., "An overview of coding tools in AV1: the first video codec from the alliance for open media," *APSIPA Transactions on Signal and Information Processing*, vol. 9, 2020.
- [16] Audio and Video Coding Standard Work-group of China, "http://www.avsc.org.cn/english/index.asp."
- [17] C.-H. Yeh, Z.-T. Zhang, M.-J. Chen, and C.-Y. Lin, "HEVC intra frame coding based on convolutional neural network," *IEEE Access*, vol. 6, pp. 50087–50095, 2018.
- [18] J. Li, B. Li, J. Xu, R. Xiong, and W. Gao, "Fully connected network-based intra prediction for image coding," *IEEE Transactions on Image Processing*, vol. 27, no. 7, pp. 3236–3247, 2018.
- [19] Z. Zhao, S. Wang, S. Wang, X. Zhang, S. Ma, and J. Yang, "Enhanced bi-prediction with convolutional neural network for High Efficiency Video Coding," *IEEE Transactions on Circuits and Systems for Video Technology*, 2018.
- [20] L. Zhao, S. Wang, X. Zhang, S. Wang, S. Ma, and W. Gao, "Enhanced motion-compensated video coding with deep virtual reference frame generation," *IEEE Transactions on Image Processing*, 2019.
- [21] S. Puri, S. Lasserre, and P. Le Callet, "CNN-based transform index prediction in multiple transforms framework to assist entropy coding," in *2017 25th European Signal Processing Conference (EUSIPCO)*. IEEE, 2017, pp. 798–802.
- [22] S. Jimbo, J. Wang, and Y. Yashima, "Deep learning-based transformation matrix estimation for bidirectional interframe

- prediction,” in *2018 IEEE 7th Global Conference on Consumer Electronics (GCCE)*. IEEE, 2018, pp. 726–730.
- [23] M. M. Alam, T. D. Nguyen, M. T. Hagan, and D. M. Chandler, “A perceptual quantization strategy for HEVC based on a convolutional neural network trained on natural images,” in *Applications of Digital Image Processing XXXVIII*. International Society for Optics and Photonics, 2015, vol. 9599, p. 959918.
- [24] R. Song, D. Liu, H. Li, and F. Wu, “Neural network-based arithmetic coding of intra prediction modes in HEVC,” in *2017 IEEE Visual Communications and Image Processing (VCIP)*. IEEE, 2017, pp. 1–4.
- [25] C. Ma, D. Liu, X. Peng, and F. Wu, “Convolutional neural network-based arithmetic coding of DC coefficients for HEVC intra coding,” in *2018 25th IEEE International Conference on Image Processing (ICIP)*. IEEE, 2018, pp. 1772–1776.
- [26] J. Lin, D. Liu, H. Yang, H. Li, and F. Wu, “Convolutional neural network-based block up-sampling for HEVC,” *IEEE Transactions on Circuits and Systems for Video Technology*, 2018.
- [27] M. Afonso, F. Zhang, and D. R. Bull, “Video compression based on spatio-temporal resolution adaptation,” *IEEE Transactions on Circuits and Systems for Video Technology*, vol. 29, no. 1, pp. 275–280, 2019.
- [28] D. Ma, F. Zhang, and D. R. Bull, “GAN-based effective bit depth adaptation for perceptual video compression,” in *2020 IEEE International Conference on Multimedia and Expo (ICME)*. IEEE, 2020, pp. 1–6.
- [29] W. Lin, X. He, X. Han, D. Liu, J. See, J. Zou, H. Xiong, and F. Wu, “Partition-aware adaptive switching neural networks for post-processing in HEVC,” *IEEE Transactions on Multimedia*, 2019.
- [30] F. Zhang, C. Feng, and D. R. Bull, “Enhancing VVC through CNN-based post-processing,” in *2020 IEEE International Conference on Multimedia and Expo (ICME)*. IEEE, 2020, pp. 1–6.
- [31] Y. Zhang, T. Shen, X. Ji, Y. Zhang, R. Xiong, and Q. Dai, “Residual highway convolutional neural networks for in-loop filtering in HEVC,” *IEEE Transactions on Image Processing*, vol. 27, no. 8, pp. 3827–3841, 2018.
- [32] C. Jia, S. Wang, X. Zhang, S. Wang, J. Liu, S. Pu, and S. Ma, “Content-aware convolutional neural network for in-loop filtering in High Efficiency Video Coding,” *IEEE Transactions on Image Processing*, vol. 28, no. 7, pp. 3343–3356, 2019.
- [33] J. Ballé, V. Laparra, and E. P. Simoncelli, “End-to-end optimized image compression,” *arXiv preprint arXiv:1611.01704*, 2016.
- [34] O. Rippel, S. Nair, C. Lew, S. Branson, A. G. Anderson, and L. Bourdev, “Learned video compression,” in *Proceedings of the IEEE International Conference on Computer Vision (ICCV)*, 2019, pp. 3454–3463.
- [35] G. Lu, W. Ouyang, D. Xu, X. Zhang, C. Cai, and Z. Gao, “DVC: An end-to-end deep video compression framework,” in *Proceedings of the IEEE Conference on Computer Vision and Pattern Recognition (CVPR)*, 2019, pp. 11006–11015.
- [36] A. Djelouah, J. Campos, S. Schaub-Meyer, and C. Schroers, “Neural inter-frame compression for video coding,” in *Proceedings of the IEEE International Conference on Computer Vision (ICCV)*, 2019, pp. 6421–6429.
- [37] A. Habibian, T. v. Rozendaal, J. M. Tomczak, and T. S. Cohen, “Video compression with rate-distortion autoencoders,” in *Proceedings of the IEEE International Conference on Computer Vision (ICCV)*, 2019, pp. 7033–7042.
- [38] Y. Zhang, S. Kwong, and S. Wang, “Machine learning based video coding optimizations: A survey,” *Information Sciences*, vol. 506, pp. 395–423, 2020.
- [39] E. Agustsson and R. Timofte, “NTIRE 2017 challenge on single image super-resolution: Dataset and study,” in *Proceedings of the IEEE Conference on Computer Vision and Pattern Recognition Workshops (CVPRW)*, July 2017.
- [40] K. Soomro, A. R. Zamir, and M. Shah, “UCF101: A dataset of 101 human actions classes from videos in the wild,” *arXiv preprint arXiv:1212.0402*, 2012.
- [41] O. Russakovsky, J. Deng, H. Su, J. Krause, S. Satheesh, S. Ma, Z. Huang, A. Karpathy, A. Khosla, M. Bernstein, et al., “Imagenet large scale visual recognition challenge,” *International Journal of Computer Vision*, vol. 115, no. 3, pp. 211–252, 2015.
- [42] D. Ma, F. Zhang, and D. R. Bull, “BVI-DVC: a training database for deep video compression,” *arXiv preprint arXiv:2003.13552*, 2020.
- [43] A. Ichigaya, S. Iwamura, and S. Nemoto, “Syntax and semantics changes of luma adaptive deblocking filter,” in *the JVET meeting*. Macao, China: ITU-T, ISO/IEC, October 2018, number JVET-L0414.
- [44] A. Kotra Meher, S. Esenlik, B. Wang, H. Gao, and E. Alshina, “Non-CE5: chroma QP derivation fix for deblocking filter (combination of JVET-P0105 and JVET-P0539),” in *the JVET meeting*. Geneva, Switzerland: ITU-T, ISO/IEC, October 2019, number JVET-P1001.
- [45] A. Browne, K. Sharman, and S. Keating, “SAO modification for 12-bit,” in *the JVET meeting*. Brussels, Belgium: ITU-T, ISO/IEC, January 2020, number JVET-Q0441.
- [46] N. Hu, V. Seregin, and M. Karczewicz, “Non-CE5: spec fix for ALF filter and transpose index calculation,” in *the JVET meeting*. Geneva, Switzerland: ITU-T, ISO/IEC, October 2019, number JVET-Q0665.
- [47] C. Dong, C. C. Loy, K. He, and X. Tang, “Image super-resolution using deep convolutional networks,” *IEEE transactions on pattern analysis and machine intelligence*, vol. 38, no. 2, pp. 295–307, 2015.
- [48] C. Dong, C. C. Loy, and X. Tang, “Accelerating the super-resolution convolutional neural network,” in *Proceedings of the European Conference on Computer Vision (ECCV)*. Springer, 2016, pp. 391–407.
- [49] J. Kim, J. Kwon Lee, and K. Mu Lee, “Accurate image super-resolution using very deep convolutional networks,” in *Proceedings of the IEEE Conference on Computer Vision and Pattern Recognition (CVPR)*, 2016, pp. 1646–1654.
- [50] Y. Tai, J. Yang, and X. Liu, “Image super-resolution via deep recursive residual network,” in *Proceedings of the IEEE Conference on Computer Vision and Pattern Recognition (CVPR)*, 2017, pp. 3147–3155.
- [51] B. Lim, S. Son, H. Kim, S. Nah, and K. Mu Lee, “Enhanced deep residual networks for single image super-resolution,” in *Proceedings of the IEEE Conference on Computer Vision and Pattern Recognition Workshops (CVPRW)*, 2017, pp. 136–144.
- [52] C. Ledig, L. Theis, F. Huszár, J. Caballero, A. Cunningham, A. Acosta, A. Aitken, A. Tejani, J. Totz, Z. Wang, et al., “Photo-realistic single image super-resolution using a generative adversarial network,” in *Proceedings of the IEEE Conference on Computer Vision and Pattern Recognition (CVPR)*, 2017, pp. 4681–4690.
- [53] Y. Zhang, K. Li, K. Li, L. Wang, B. Zhong, and Y. Fu, “Image super-resolution using very deep residual channel attention networks,” in *Proceedings of the European Conference on Computer Vision (ECCV)*, 2018, pp. 286–301.
- [54] D. Ma, M. F. Afonso, F. Zhang, and D. R. Bull, “Perceptually-inspired super-resolution of compressed videos,” in *Applications of Digital Image Processing XLII*. International Society for Optics and Photonics, 2019, vol. 11137, pp. 310–318.
- [55] Y. Zhang, Y. Tian, Y. Kong, B. Zhong, and Y. Fu, “Residual dense network for image super-resolution,” in *Proceedings of the IEEE Conference on Computer Vision and Pattern Recognition (CVPR)*, 2018, pp. 2472–2481.
- [56] X. Wang, K. Yu, S. Wu, J. Gu, Y. Liu, C. Dong, Y. Qiao, and C. Change Loy, “ESRGAN: Enhanced super-resolution generative adversarial networks,” in *Proceedings of the European Conference on Computer Vision (ECCV)*, 2018, pp. 0–0.
- [57] N. Ahn, B. Kang, and K.-A. Sohn, “Fast, accurate, and

- lightweight super-resolution with cascading residual network,” in *Proceedings of the European Conference on Computer Vision (ECCV)*, 2018, pp. 252–268.
- [58] N. Ahn, B. Kang, and K.-A. Sohn, “Photo-realistic image super-resolution with fast and lightweight cascading residual network,” *arXiv preprint arXiv:1903.02240*, 2019.
- [59] Y. Wang, H. Zhu, Y. Li, Z. Chen, and S. Liu, “Dense residual convolutional neural network based in-loop filter for HEVC,” in *2018 IEEE Visual Communications and Image Processing (VCIP)*. IEEE, 2018, pp. 1–4.
- [60] L. Ma, Y. Tian, P. Xing, and T. Huang, “Residual-based post-processing for HEVC,” *IEEE MultiMedia*, vol. 26, no. 4, pp. 67–79, 2019.
- [61] H. Zhao, M. He, G. Teng, X. Shang, G. Wang, and Y. Feng, “A CNN-based post-processing algorithm for video coding efficiency improvement,” *IEEE Access*, 2019.
- [62] F. Zhang, M. Afonso, and D. R. Bull, “ViSTRA2: Video coding using spatial resolution and effective bit depth adaptation,” *arXiv preprint arXiv:1911.02833*, 2019.
- [63] D. Bull, F. Zhang, and M. Afonso, “Description of SDR video coding technology proposal by University of Bristol,” in *the JVET meeting*. San Diego, US: ITU-T, ISO/IEC, April 2018, number JVET-J0031.
- [64] H. Yin, R. Yang, X. Fang, and S. Ma, “CE10-1.7: Adaptive convolutional neural network loop filter,” in *the JVET meeting*. Gothenburg, Sweden: ITU-T, ISO/IEC, July 2019, number JVET-O0063.
- [65] S. Wan, M. Wang, Y. Ma, J. Huo, H. Gong, C. Zou, and et al., “CE10: Integrated in-loop filter based on cnn (Tests 2.1, 2.2 and 2.3),” in *the JVET meeting*. Gothenburg, Sweden: ITU-T, ISO/IEC, July 2019, number JVET-O0079.
- [66] Y. Kidani, K. Kawamura, K. Unno, and S. Naito, “CE10-1.10/CE10-1.11: Evaluation results of CNN-based filtering with on-line learning model,” in *the JVET meeting*. Gothenburg, Sweden: ITU-T, ISO/IEC, July 2019, number JVET-O0131.
- [67] Y. Kidani, K. Kawamura, K. Unno, and S. Naito, “CE10-2.10/CE10-2.11: Evaluation results of CNN-based filtering with off-line learning model,” in *the JVET meeting*. Gothenburg, Sweden: ITU-T, ISO/IEC, July 2019, number JVET-O0132.
- [68] Y.-L. Hsiao, O. Chubach, C.-Y. Chen, T.-D. Chuang, C.-W. Hsu, Y.-W. Huang, and et al., “CE10-1.2: convolutional neural network loop filter,” in *the JVET meeting*. Gothenburg, Sweden: ITU-T, ISO/IEC, July 2019, number JVET-O0056.
- [69] Y. Wang, T. Ouyang, C. Zou, Y. Li, and Z. Chen, “CE10: dense residual convolutional neural network based in-loop filter (Tests 2.5 and 2.7),” in *the JVET meeting*. Gothenburg, Sweden: ITU-T, ISO/IEC, July 2019, number JVET-O0101-v2.
- [70] M.-Z. Wang, S. Wan, H. Gong, and M.-Y. Ma, “Attention-based dual-scale CNN in-loop filter for Versatile Video Coding,” *IEEE Access*, vol. 7, pp. 145214–145226, 2019.
- [71] D. Liu, Z. Wang, Y. Fan, X. Liu, Z. Wang, S. Chang, and T. Huang, “Robust video super-resolution with learned temporal dynamics,” in *Proceedings of the IEEE International Conference on Computer Vision (ICCV)*, 2017, pp. 2507–2515.
- [72] K. He, X. Zhang, S. Ren, and J. Sun, “Deep residual learning for image recognition,” in *Proceedings of the IEEE Conference on Computer Vision and Pattern Recognition (CVPR)*, 2016, pp. 770–778.
- [73] T. Dai, J. Cai, Y. Zhang, S.-T. Xia, and L. Zhang, “Second-order attention network for single image super-resolution,” in *Proceedings of the IEEE Conference on Computer Vision and Pattern Recognition (CVPR)*, 2019, pp. 11065–11074.
- [74] G. Huang, Z. Liu, L. Van Der Maaten, and K. Q. Weinberger, “Densely connected convolutional networks,” in *Proceedings of the IEEE Conference on Computer Vision and Pattern Recognition (CVPR)*, 2017, pp. 4700–4708.
- [75] D. P. Kingma and J. Ba, “Adam: a method for stochastic optimization,” *arXiv preprint arXiv:1412.6980*, 2014.
- [76] G. Bjøntegaard, “Calculation of average PSNR differences between RD-curves,” in *13th VCEG Meeting, no. VCEG-M33, Austin, Texas*, 2001, pp. USA: ITU-T.
- [77] Z. Li, A. Aaron, I. Katsavounidis, A. Moorthy, and M. Manohara, “Toward a practical perceptual video quality metric,” *The Netflix Tech Blog*, vol. 6, 2016.
- [78] F. Zhang, F. M. Moss, R. Baddeley, and D. R. Bull, “BVI-HD: A video quality database for HEVC compressed and texture synthesized content,” *IEEE Transactions on Multimedia*, vol. 20, no. 10, pp. 2620–2630, 2018.
- [79] BlueCrystal Phase 4, ,” <https://www.acrc.bris.ac.uk/protected/bc4-docs/>.
- [80] X. Zhang, R. Xiong, W. Lin, J. Zhang, S. Wang, S. Ma, and W. Gao, “Low-rank-based nonlocal adaptive loop filter for high-efficiency video compression,” *IEEE Transactions on Circuits and Systems for Video Technology*, vol. 27, no. 10, pp. 2177–2188, 2016.
- [81] R. K. Srivastava, K. Greff, and J. Schmidhuber, “Highway networks,” *arXiv preprint arXiv:1505.00387*, 2015.
- [82] R. K. Srivastava, K. Greff, and J. Schmidhuber, “Training very deep networks,” in *Advances in neural information processing systems*, 2015, pp. 2377–2385.
- [83] X. Qin, Z. Zhang, C. Huang, M. Dehghan, O. R. Zaiane, and M. Jagersand, “U²-Net: going deeper with nested U-structure for salient object detection,” *Pattern Recognition*, vol. 106, pp. 107404, 2020.
- [84] F. Zhang, M. Afonso, and D. R. Bull, “Enhanced video compression based on effective bit depth adaptation,” in *2019 IEEE International Conference on Image Processing (ICIP)*. IEEE, 2019, pp. 1720–1724.
- [85] Y. Li and S. Liu, “Bog report on neural networks for video coding,” in *the JVET meeting*. Marrakech, Morocco: ITU-T, ISO/IEC, Jan 2019, number JVET-M0904.